




# Carboxymethyl Cellulose-Amuniacum Gum Based Edible Films Enriched with Clove Essential Oil: Optimization Formulation Using Response Surface Methodology (RSM)

A. Homayouni Rad<sup>1</sup>, K. Arab<sup>2</sup>, A. Berri<sup>2</sup>, T. Fazeliioskouei<sup>3</sup>, B. Ebrahimi<sup>4\*</sup> 

1. Department of Food Science and Technology, Faculty of Nutrition and Food Sciences, Tabriz University of Medical Sciences, Tabriz, Iran

2. Department of Food Science and Technology, Faculty of Agriculture, University of Tabriz, Tabriz, Iran

3. Student research committee, Department of food science and technology, Faculty of Nutrition and Food Sciences, Tabriz University of Medical Sciences, Tabriz, Iran

4. Department of Food Science and Technology, Maragheh University of Medical Sciences, Maragheh, Iran

## HIGHLIGHTS

- Combined effect of Carboxymethyl Cellulose (CMC), Amuniacum Gum (AMG), and Clove Essential Oil (CEO) on physical properties of CMC-AMG films was investigated.
- Optimization was aimed to maximize Whiteness Index, Ultimate Tensile Strength, and Strain at Break, and minimize total color difference ( $\Delta E$ ) values.
- Films with highest Ultimate Tensile Strength obtained with 5 g CMC, 1.5 g AMG, and 15% CEO.
- Highest Strain at Break achieved with 5 g CMC, 1 g AMG, and 30% CEO.
- Addition of CEO increased antimicrobial activity against *Salmonella*, *Pseudomonas*, *Escherichia coli*, and *Listeria*.

## Article type

Original article

## Keywords

Edible Films  
Oils, Volatile  
Carboxymethyl Cellulose  
Sodium  
Spectroscopy, Fourier  
Transform Infrared

## Article history

Received: 1 Jun 2023

Revised: 13 Sep 2023

Accepted: 30 Nov 2023

## Acronyms and abbreviations

AMG=Amuniacum Gum  
CEO=Clove Essential Oil  
CMC=Carboxymethyl Cellulose  
DSC=Differential Scanning  
Calorimeter  
FTIR=Fourier Transform Infrared  
Spectroscopy  
RSM=Response Surface  
Methodology  
SB=Strain at Break  
SEM=Scanning Electron  
Microscope  
UTS=Ultimate Tensile Strength  
WI=Whiteness Index

## ABSTRACT

**Background:** Polysaccharides, particularly Carboxymethyl Cellulose (CMC) and Ammoniacum Gum (AMG), are considered valuable due to their thermal stability and non-toxicity. CMC has good film-forming ability but weak mechanical properties, while AMG shows promise with its unique chemical composition. Additionally, essential oils, such as Clove Essential Oil (CEO), are being used to enhance the antimicrobial properties of edible films, offering a natural way to extend the shelf life of food products.

**Methods:** This study investigated the combined effect of CMC: 0.5-1.5 wt %, AMG: 1-5 wt %, as well as CEO: 0-30 v/v % on the physical characteristics of the CMC-AMG films by Response Surface Methodology. The optimization was performed with the aim of maximizing Whiteness Index, Ultimate Tensile Strength (UTS), and Strain at Break (SB) and minimizing total color difference ( $\Delta E$ ) values. Fourier-Transform Infrared Spectroscopy, film microstructure, Differential Scanning Calorimeter analysis, and antibacterial activity were investigated. The analysis was conducted using Design Expert software version 10.00 (STAT-EASE Inc., Minneapolis, USA).

**Result:** The films with the highest UTS have been obtained through a composition of 5 g CMC, 1.5 g AMG, and 15% CEO. On the contrary, using a composition of 5 g CMC, 1 g AMG, and 30% CEO revealed the highest SB (115.41%). The highest UTS value of 13.17 MPa was obtained with a formulation consisting of 5% AMG, 1.5% CMC, and 15% CEO. Nevertheless, the maximum SB value of 115.41% was achieved with a formulation containing 5% AMG, 1% CMC, and 30% CEO. Moreover, heterogeneous microstructure and more opaque films were obtained as identified by the higher  $\Delta E$ . The Differential Scanning Calorimeter results demonstrated that incorporating a CEO did not impinge on thermal stability. Furthermore, the addition of CEO led to a rise in antimicrobial activity against *Salmonella enterica*, *Pseudomonas fluorescens*, *Escherichia coli*, and *Listeria monocytogenes*.

**Conclusion:** In conclusion, combination of CMC and AMG in optimum levels, led to the production of a film with acceptable mechanical properties. Also, these films showed significant antimicrobial activity.

© 2023, Shahid Sadoughi University of Medical Sciences. This is an open access article under the Creative Commons Attribution 4.0 International License.

\* Corresponding author (B. Ebrahimi)

E-mail: ebrahimib@tbzmed.ac.ir

ORCID ID: <https://orcid.org/0000-0002-5278-0841>

**To cite:** Homayouni Rad A., Arab K., Berri A., Fazeliioskouei T., Ebrahimi B. (2023). Carboxymethyl cellulose-amuniacum gum based edible films enriched with clove essential oil: optimization formulation using response surface methodology (RSM). *Journal of Food Quality and Hazards Control*. 10: 199-210.

## Introduction

To extend the food's shelf life or preserve its quality during the storage period and commercialization, the use of packaging has been extremely noteworthy. Current use of plastic packaging materials have proven to be very detrimental against the environment owing to toxicity and their persistency. Indirect additives and monomers including cadmium, phthalates, and bisphenol A can potentially transfer from packaging materials into the food, extremely dangerous for the consumer's health (Yeddes et al., 2020). Therefore, there is a critical need to design and manufacture safe, biodegradable, and eco-friendly packaging materials from polysaccharides, proteins, and lipids.

Among all the naturally derived polymers, polysaccharides are considered as valuable ingredients related to their satisfactory thermal stability, non-toxicity, abundance, being biodegradable, and affordable cost (Ebrahimi et al., 2018). Carboxymethyl Cellulose (CMC) appears to be an anionic water-soluble derivative of cellulose that bears appropriate ability to form transparent films (Akhtar et al., 2018). It is colorless, toxicologically harmless, a preferred substitution for the prepare CMC-protein blend films due to a good compatibility with the protein, and a good barrier against carbon dioxide, oxygen, and lipids; nonetheless, it exhibits weak mechanical properties (Azarifar et al., 2019; Ghanbarzadeh and Almasi, 2011). Due to the presence of many hydrophilic moieties, CMC bears high water vapor permeability and water binding capability, and constitutes a gel during heating. CMC films fail to possess any intrinsic antimicrobial attributes (Raeisi et al., 2015).

Amuniacum Gum (AMG) is released under severe stress conditions by stems and leaves of plants *Dorema ammoniacum* D. Don (Umbelliferae), which chiefly grow in central and eastern of Iran and traditionally deployed for the treatment of anthelmintic and stomach disorders (Ebrahimi et al., 2020). Few studies have been devoted to investigate AMG. From a chemical viewpoint, AMG is regarded as an anionic hydrocolloid characterized by low protein content, and high levels of galactose and arabinose. It demonstrates superior surface and interface activity with a molecular weight of 35 kDa, compared to gum Arabic. Structural analysis of AMG discloses the existence of a backbone constituted by  $\beta$ -D-Galp residues, primarily branched via 4-O-methyl- $\alpha$ -D-glucopyranosyl units (Ebrahimi et al., 2022).

Essential Oils (EOs), identified as plant secondary metabolites, exhibit exceptional antimicrobial and antifungal properties. Currently, edible films infused with EOs are observed as a potent and innovative strategy to prolong the shelf life of various food items (Ju et al., 2019). Clove Essential Oil (CEO) appears to be an

attractive compound with great potential for application as natural food preservatives. The high content of eugenol in the CEO is mainly responsible for its biological and antimicrobial activity by damaging cell membranes phospholipids and cellular proteins. Moreover, various therapeutic effects, including anticarcinogenic, antispasmodic, antivomiting, antiphlogistic, analgesic, antiseptic, and kidney reinforcement have been found (Gülçin et al., 2004).

Response Surface Methodology (RSM) has turned out to be a mathematical modeling for the design of experiments which clarifies the relationship between response of interest and multiple variables. One of the chief advantages of using RSM in film formulation is that it diminishes the number of required experimental runs (Bezerra et al., 2008). This study aimed to find the best proportion using the mixture design and to investigate the microstructural, Fourier-Transform Infrared Spectroscopy (FTIR) analysis, physical properties, and antimicrobial features of a novel biodegradable film made of CMC and AMG containing CEO, as an active component.

## Materials and methods

### Materials

CMC, which possesses a viscosity ranging from 1,500 to 3,500 centipoises in a 1% solution in water at 20 °C, a pKa of 3.5, and a molecular weight of 41,000 g/mol, was procured from Merck, Germany. Additional materials included were as follows: AMG (extraction and purification protocol of the gum was implemented according to the performance of Ebrahimi et al. (2022), CEO (Johare Taem Shargh, Mashhad, Iran), glycerol (Merck Co., Darmstadt, Germany). Chemicals and other supplies were obtained from Merck, Germany.

### Experimental design

In the current study, RSM deployed to investigate the effects of AMG concentration ( $X_1$ : 1-5 wt %), CMC concentration ( $X_2$ : 0.5-1.5 wt %), and CEO concentration ( $X_3$ : 0-30 v/v %) on the dependent variables of the films in Food Biophysics Laboratory of Tabriz University Laboratory. The declared variables comprised Ultimate Tensile Strength (UTS) (MPa), Strain at Break (SB) (%), and color properties (total color difference ( $\Delta E$ ) and Whiteness Index (WI)). Totally, 17 formulations were studied with five replications at the center points to calculate repeatability and accuracy of the data. The experimental design matrix is demonstrated in Table 1. In spite of transferring the effects of uncontrollable factors, we randomized the experimental sequence. Data were analyzed by matching to a second order as a dependent

variables equation (1):

$$Y = \beta_0 + \sum_{i=1}^k \beta_i X_i + \sum_{i=1}^k \beta_{ii} X_i^2 + \sum_{i=1}^{k-1} \sum_{j=2}^k \beta_{ij} X_i X_j + \varepsilon \quad (1)$$

Y is obtained as the predicted response,  $\beta_0$  is determined as the constant coefficient,  $\beta_i$  are the linear coefficients,  $\beta_{ii}$  represent the quadratic coefficients,  $\beta_{ij}$  illustrate the interaction coefficients,  $X_i$  and  $X_j$  are independent variables and ultimately  $\varepsilon$  represents the error associated with the predicted response (Yeddes et al., 2020).

#### Preparation of biodegradable emulsion films

First, 1-5% of AMG and 0.5-1.5% of CMC (Ebrahimi et al., 2022) were dissolved separately in 50 ml of distilled water at 80 °C and mixed for 30 min with a mixer (HMS., Iran), later mixed. Glycerol (dry basis of hydrocolloid) was added as plasticizer to solution and stirred for 10 min at 80 °C; then the mixture was cooled to 60 °C as well. To produce emulsion films, Tween-80 (half concentration of CEO) as emulsifier was added to the 20 ml of water and homogenized for 1 min at 20,000 rpm. Prepared Tween-80 solution blended for 6 min with 0-30% CEO (based on dry gum) at 20,000 rpm by UltraTax (IKA Dispersers T 25 digital ULTRA- TURRAX). Eventually, the film was prepared by blending two prepared solutions for 60 min at 60 °C and the solutions were poured in a teflon coated petri dishes and dried for 24 h at 37 °C. Film specimens were removed from the dishes and stored at 25 °C with relative humidity of 50% (RH) for additional measurement (Walid et al., 2022).

#### Film characterization

##### -Film thickness

The thickness of the films samples was considered using a handheld digital micrometer (Alton M820-25, China). The average thickness was measured at least from 10 various randomly locations around each film (Walid et al., 2022).

##### -Mechanical properties of films

The mechanical characteristics of the films, namely UTS and SB, were investigated with a texture analyzer (TA.XT Stable Micro 164 System, UK) in line with the ASTM D882-02 (2002) procedure. Before testing, the film samples had been conditioned in a desiccator and subsequently chopped into pieces of 1.5×10 cm. Tensile testing was accomplished with specific self-tightening roller grips (Mahar Fan Azbar Co. Iran). The initial grip-to-grip distance was fixed at 50 mm and the test speed was set at 5 mm/min. Eventually, the mechanical properties were explored through the mean thickness of each test sample and all measurements were repeated at least three times (Ebrahimi et al., 2018).

##### -Color analysis

The films' color changes were evaluated using a Minolta colorimeter from Japan. The assessment employed International Commission on Illumination (CIE) Lab parameters, including  $a^*$  (red-green),  $L^*$  (black-white), and  $b^*$  (yellow-blue). To calibrate these parameters, a white standard plate was used as the background, with values of  $L^*=94.26$ ,  $a^*=0.36$ , and  $b^*=0.16$ . Film's  $\Delta E$  and WI were also calculated by using following equations 2 and 3 (Ghanbarzadeh and Almasi, 2011):

$$\Delta E = \sqrt{(\Delta L^*)^2 + (\Delta a^*)^2 + (\Delta b^*)^2} \quad (2)$$

$$WI = 100 - \sqrt{(100 - L^*)^2 + a^{*2} + b^{*2}} \quad (3)$$

$\Delta L^*$ ,  $\Delta a^*$ , and  $\Delta b^*$  are correspond to the difference between the color of white standard plate and the color parameter of film.

#### -Optimization

The optimal production conditions were determined using the maximum UTS, SB, WI and the minimum  $\Delta E$ . CMC and AMG concentrations were considered within the range.

#### Film microstructure

The surface and cross-sectional morphologies of the films were analyzed with a Scanning Electron Microscope (SEM) model ZEISS LEO-1430 VP from the UK. To prepare the samples for imaging, they were fixed onto a sample holder and coated with a layer of gold. Micrographs of the samples were obtained at a voltage of 5 kV.

#### FTIR

The microstructure and functional group interactions of films were characterized by FTIR spectrophotometer (Perkin-Elmer B25, Paris Area, France). The spectra of each film have been scanned from 4,000 to 400 1/cm with a resolution of 4 1/cm (Salama et al., 2019).

#### Thermal properties

Thermodynamic features of films were determined from Differential Scanning Calorimeter (DSC) TA DSC Q200 (New Castle, USA). About 5-7 mg of film samples were hermetically accumulated in aluminum DSC pans, an identical empty pan served as source in each test. The specimens were heated up to 300 °C at a rate of 10 °C/min. The experiments were repeated in three times (Kadzińska et al., 2020).

#### Antibacterial properties of films

Antibacterial test including disc diffusion assay was accomplished to regard the inhibitory effect of films against food pathogenic bacteria (including *Escherichia*

*coli* O157: H7 (NCTC 12900), *Salmonella enterica* (ATCC 14028), *Pseudomonas fluorescens* (NCTC 10038), and *Listeria monocytogenes* (ATCC 7644) (Pereda et al., 2011). For disc diffusion assay, the film samples were punched to 1 cm in diameter discs and then situated in direct contact with the Müller Hinton agar plates (Merck, Darmstadt, Germany). In advance of this procedure, 0.1 ml of  $10^5$ – $10^6$  Colony Forming Unit (CFU)/ml bacterial suspension was added to plates and afterwards incubated at 37 °C for a duration of 24 h. An accurately digital caliper (INSTAR, China) was utilized for exploring the diameter (mm) of the non-growth halo zone (Azarifar et al., 2019). To study a probable antimicrobial effect of the CMC-AMG films without additives, we applied pure CMC-AMG film without any CEO as control.

#### Statistical analyses

The experimental design, response surface plotting, and also regression analysis of the test results were conducted using Design Expert software, notably version 10.00 (STAT-EASE Inc., Minneapolis, USA). The software facilitated the development of analysis of variance (ANOVA) tables, permitting for the measurement of individual and interactive effects of the model output.

## Results

#### Thickness

The thickness of enriched CMC-AMG films with CEO was ranged from 0.05 to 0.15 mm and significantly ( $p < 0.05$ ) increased with a raise in the contents of the CMC and AMG (Table 1). Furthermore, the thickness of films failed to impress significantly by incorporating the CEO.

#### Mechanical properties

We presented 3D response surface plots for utilization of an independent variable's (CMC, AMG, and CEO concentrations) impact and interactions on an outcome variable (UTS and SB) (Figure 1). Incorporation of CEO triggered a reduction at the UTS of the CMC-AMG films. Pure CMC-AMG film had UTS from 6.17 to 11.78 MPa. An increase level in the CEO from 0 to 30% w/w significantly diminished the UTS to 4.32 MPa (Figure 1: a). The SB value increased from 63.78 to 115.41% accompanied with the raise in the CEO and AMG in the film, attributable to higher flexibility and lower rigidity. On the contrary, it reduced with the increasing concentration of CMC (Figure 1: b).

#### Color properties

To illustrate the effect of combined variables on  $\Delta E$  and WI values of the CMC-AMG films enriched with CEO, 3D response surfaces plots were considered in Figure 2. The

$\Delta E$  values increased with a heightening in the CMC, AMG, and CEO concentrations. The maximum  $\Delta E$  value (16.01) was obtained at 1% CMC, 5% AMG, and 30% CEO. In contrast, WI decreased as AMG and CEO concentration raised, while being increased slightly by increasing CMC ones. By increasing CEO concentration up to 30%, a reduction was observed in the amount of WI from 51.12 to 47.93, therefore the composite films became opaquer.

#### Optimization

To achieve the desirable properties of the prepared films, optimization was accomplished using Design Expert software (version 10.0.7.0). The data analysis identified that the optimum blend for producing the CMC-AMG film enriched with CEO was uncovered to be 1.5% CMC, 4.5% AMG, and 14.19% CEO.

#### Verification

To validate the appropriateness and sufficiency of the model for predicting optimal conditions, a model of accuracy test was utilized. The proximity of the predicted values to the experimental data signified the appropriateness and acceptance of the model. According to the test results illustrated in Table 4, the model highlighted a strong capability to predict accurately.

#### Microstructural and spectroscopy analysis

##### -FTIR

FTIR spectroscopy was used to detect specific chemical groups in the structure of food components. The FTIR spectra of CMC-AMG films containing 0, 15, and 30% CEO are demonstrated in Figure 3.

##### -SEM

Figure 4 illustrates the morphologies of the surface and cross sections of CMC-AMG films with the addition of CEO. Based on the results, control CMC-AMG film surface (Figure 4: a) was uniform and smooth with no material accumulation, protrusions, and bubbles. Furthermore the images of cross section disclosed that the sheets densely layer-stacked. This status implies a close compatibility and interaction between CMC and AMG biopolymers. With the incorporation of oil into film formulation (Figure 4: b, c), the uniformity and cohesion became looser, resulting in the formation of micro-cavities and rough surface in the films incorporated with 15 and 30% CEO.

##### DSC

Figure 5 unveils the thermal features of films derived from AMG-CMC gum incorporated with various concentrations of CEO. According to this Figure, it seems to be noticeable that the melting peak of the control film



appeared at a temperature of 181.37 °C. However, this peak increased to 196.62 and 201.97 °C in films that involved 15 and 30% of CEO, respectively.

#### Antibacterial activity of films incorporated with CEO

Figure 6 illustrates the antimicrobial traits of CMC-AMG films containing CEO against *S. enterica*, *P. fluorescens*, *E. coli*, as well as *L. monocytogenes* bacteria. It is apparent from the image that the control film failed to exhibit any zones of inhibition against these four pathogenic bacteria.

This status denotes that the CMC-AMG film itself, without the incorporation of CEO, failed to bear inherent antimicrobial activity against these distinct bacteria. For all the tested bacterial strains, increasing CEO concentration reveals significant and increased diameter of inhibition zones. With raising the concentration CEO from 10 to 30 %, the inhibitory zones against *S. enterica*, *P. fluorescens*, *E. coli*, as well as *L. monocytogenes* enhanced from 19.63 to 28.55 mm, 16.32 to 21.36 mm, 14.65 to 22.74 mm, and 21.36 to 32.50 mm, respectively.

**Table 1:** Experimental design and responses of the mixture design.

| Thickness*                | Responses      |                |                |                | Proportions of components |                |                | Film samples |
|---------------------------|----------------|----------------|----------------|----------------|---------------------------|----------------|----------------|--------------|
|                           | Y <sub>4</sub> | Y <sub>3</sub> | Y <sub>2</sub> | Y <sub>1</sub> | X <sub>3</sub>            | X <sub>2</sub> | X <sub>1</sub> |              |
|                           | WI             | ΔE             | SB (%)         | UTS (MPa)      | CEO                       | CMC            | AMG            |              |
| 0.09 <sup>ef</sup> ±0.11  | 49.1           | 14.12          | 80.29          | 7.63           | 15                        | 1              | 3              | F1           |
| 0.08 <sup>gh</sup> ±0.16  | 49.21          | 14.98          | 84.32          | 8.41           | 15                        | 1              | 3              | F2           |
| 0.07 <sup>hi</sup> ±0.21  | 50.63          | 12.78          | 92.12          | 7.63           | 0                         | 0.5            | 3              | F3           |
| 0.05 <sup>i</sup> ±0.13   | 49.03          | 14.51          | 82.72          | 5.01           | 15                        | 0.5            | 1              | F4           |
| 0.09 <sup>efg</sup> ±0.14 | 48.93          | 14.34          | 81.98          | 7.76           | 15                        | 1              | 3              | F5           |
| 0.1 <sup>e</sup> ±0.12    | 49.23          | 14.36          | 89.19          | 10.53          | 0                         | 1              | 5              | F6           |
| 0.15 <sup>a</sup> ±0.22   | 48.43          | 15.94          | 91.1           | 13.17          | 15                        | 1.5            | 5              | F7           |
| 0.06 <sup>i</sup> ±0.1    | 48.21          | 15.33          | 94.21          | 4.32           | 30                        | 1              | 1              | F8           |
| 0.07 <sup>hi</sup> ±0.08  | 47.93          | 15.62          | 104.12         | 5.43           | 30                        | 0.5            | 3              | F9           |
| 0.08 <sup>gh</sup> ±0.16  | 48.78          | 14.13          | 82.67          | 7.3            | 15                        | 1              | 3              | F10          |
| 0.09 <sup>fg</sup> ±0.13  | 48.91          | 14.23          | 86.13          | 7.38           | 15                        | 1              | 3              | F11          |
| 0.11 <sup>d</sup> ±0.09   | 49.23          | 14.84          | 74.51          | 10.21          | 15                        | 1.5            | 1              | F12          |
| 0.1 <sup>e</sup> ±0.06    | 48.21          | 16.01          | 115.41         | 8.91           | 30                        | 1              | 5              | F13          |
| 0.13 <sup>c</sup> ±0.09   | 50.91          | 13.14          | 66.15          | 11.78          | 0                         | 1.5            | 3              | F14          |
| 0.07 <sup>hi</sup> ±0.22  | 47.99          | 15.62          | 100.76         | 8.05           | 15                        | 0.5            | 5              | F15          |
| 0.14 <sup>b</sup> ±0.19   | 48.78          | 15.33          | 97.2           | 8.87           | 30                        | 1.5            | 3              | F16          |
| 0.06 <sup>i</sup> ±0.15   | 51.12          | 13.98          | 63.78          | 6.17           | 0                         | 1              | 1              | F17          |

\*Values are expressed as mean±standard deviation. Different letters in the same column indicate significantly different ( $p \leq 0.05$ ). Carboxymethyl Cellulose (CMC), Amuniacum Gum (AMG), Clove Essential Oil (CEO), Whiteness Index (WI), Ultimate Tensile Strength (UTS), and Strain at Break (SB), total color difference (ΔE).

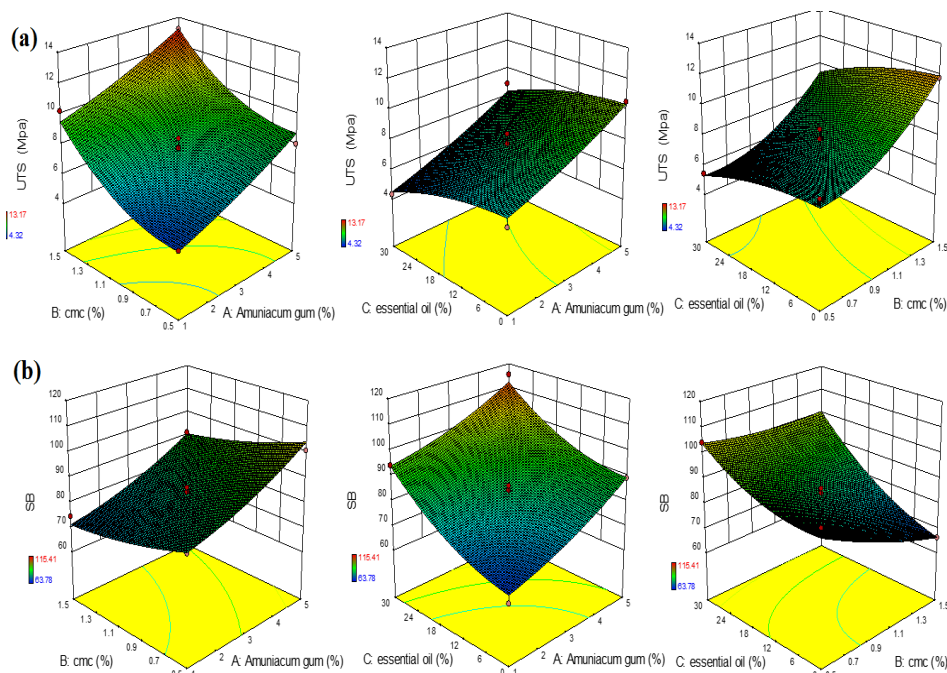


**Figure 1:** Response surface plots for the effects of Carboxymethyl Cellulose (CMC), Amuniacum Gum (AMG), and Clove Essential Oil (CEO) in composite films on mechanical properties for Ultimate Tensile Strength (UTS) (a), and Strain at Break (SB) (b)

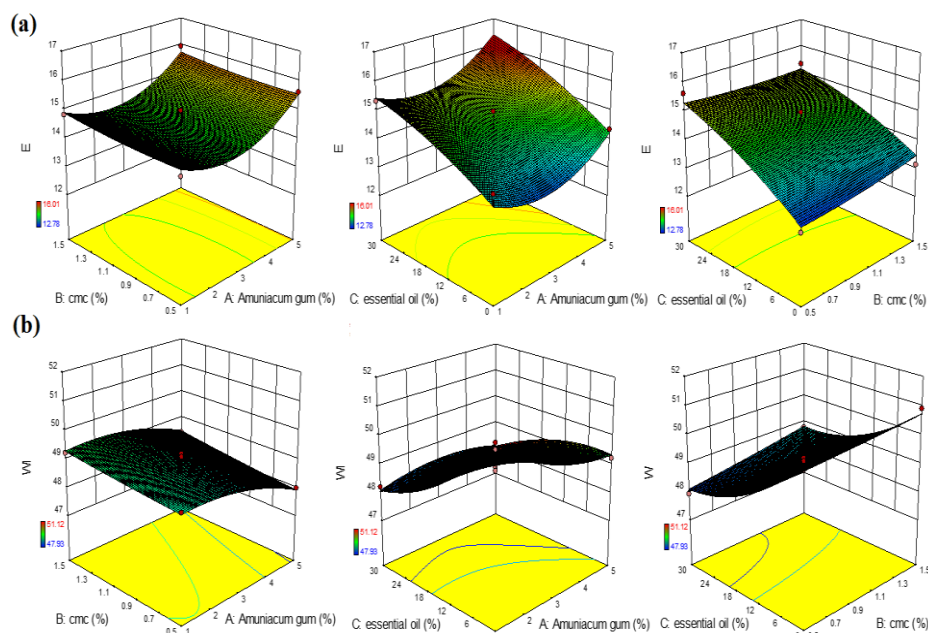


**Figure 2:** Response surface plots for the effects of Carboxymethyl Cellulose (CMC), Amuniacum Gum (AMG), and Clove Essential Oil (CEO) in composite films on color properties for total color difference ( $\Delta E$ ) (a), and Whiteness Index (WI) (b)

**Table 2:** The statistical results of the fitted model (reduced to the second degree)

| Response   | Mean  | SD   | CV   | $R^2$ | $R^2_{\text{adjusted}}$ |
|------------|-------|------|------|-------|-------------------------|
| UTS (MPa)  | 8.15  | 0.67 | 8.20 | 0.96  | 0.91                    |
| SB (%)     | 87.45 | 3.57 | 4.08 | 0.96  | 0.92                    |
| $\Delta E$ | 14.66 | 0.42 | 2.86 | 0.90  | 0.79                    |
| WI         | 49.09 | 0.19 | 0.38 | 0.98  | 0.96                    |

WI=Whiteness Index; UTS=Ultimate Tensile Strength; SB=Strain at Break;  $\Delta E$ =Total Color Difference

**Table 3:** The appropriate models correctly predict the process in a coded form.

| Response   | Models                                                                                                        |
|------------|---------------------------------------------------------------------------------------------------------------|
| UTS (MPa)  | $UTS (MPa) = +7.70 + 1.87A + 2.24B - 1.07C - 0.020AB + 0.058AC - 0.18BC + 0.23A^2 + 1.18B^2 - 0.45C^2$        |
| SB (%)     | $SB (\%) = +83.08 + 10.16A - 6.34B + 12.46C - 0.36AB - 1.05AC + 4.76BC + 2.47A^2 + 1.72B^2 + 5.10C^2$         |
| $\Delta E$ | $\Delta E = +14.36 + 0.41A + 0.090B + 1.00C - 2.500E-003AB + 0.075AC - 0.16BC + 0.78A^2 + 0.082B^2 - 0.22C^2$ |
| WI         | $WI = +48.99 - 0.47A + 0.22B - 1.09C + 0.060AB + 0.47AC + 0.14BC - 0.34A^2 + 0.027B^2 + 0.55C^2$              |

WI=Whiteness Index; UTS=Ultimate Tensile Strength; SB=Strain at Break;  $\Delta E$ =Total Color Difference  
A=Amuniacum Gum; B=Carboxymethyl Cellulose; C=Clove Essential Oil

**Table 4:** Predicted and actual values of responses under optimal film production conditions

| Response   | Predicted | Actual values |
|------------|-----------|---------------|
| UTS (MPa)  | 9.14      | 9.25          |
| SB (%)     | 102.58    | 101.22        |
| $\Delta E$ | 14.08     | 14.06         |
| WI         | 49.23     | 48.12         |

WI=Whiteness Index; UTS=Ultimate Tensile Strength; SB=Strain at Break;  $\Delta E$ =Total Color Difference

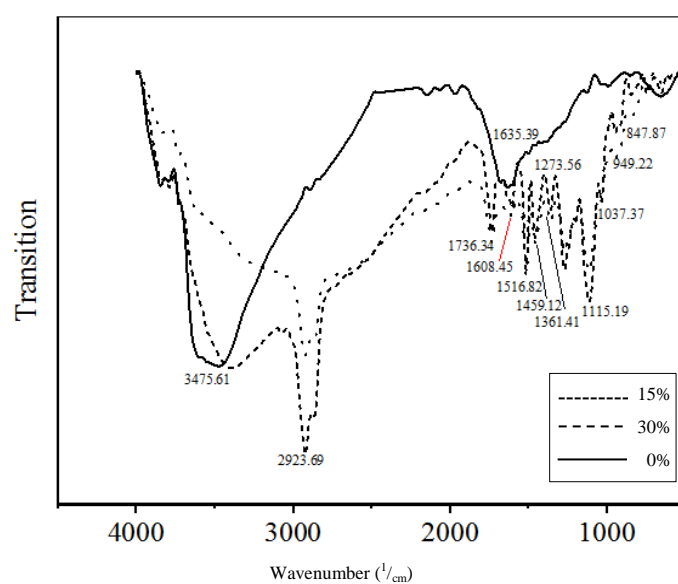


**Figure 3:** Fourier-transform Infrared Spectroscopy (FTIR) of Carboxymethyl Cellulose (CMC)-Amuniacum Gum (AMG) films containing 0, 15, and 30% Clove Essential Oil (CEO)

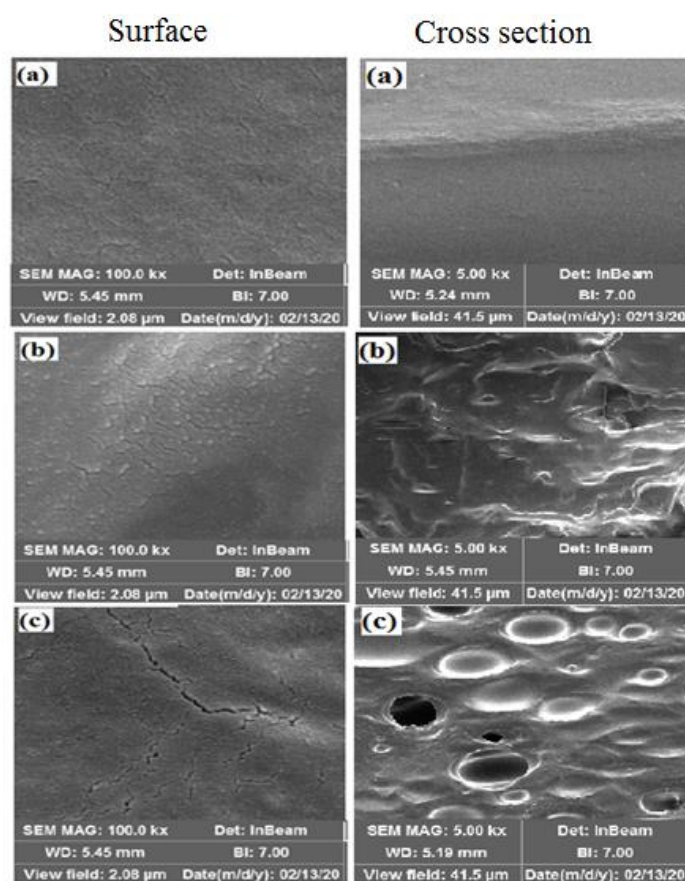


**Figure 4:** Film microstructure of Carboxymethyl Cellulose (CMC)-Amuniacum Gum (AMG) enriched with (a) 0%, (b) 15%, and (c) 30% Clove Essential Oil (CEO)

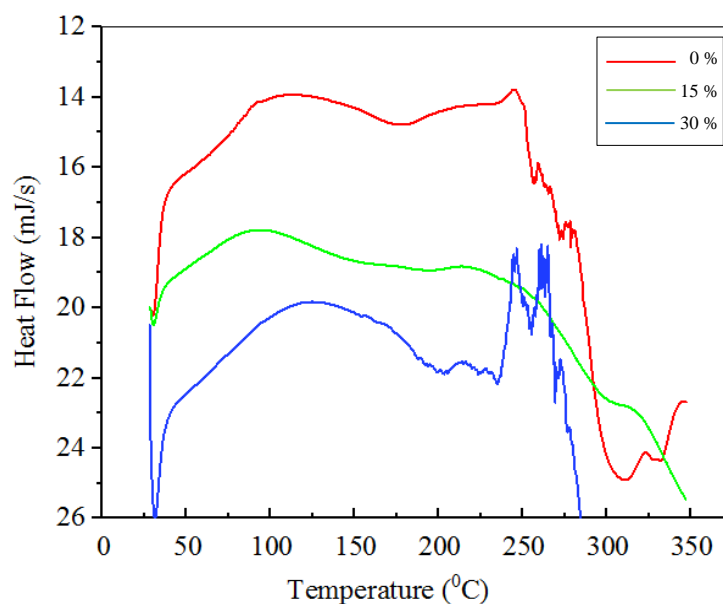


**Figure 5:** Differential Scanning Calorimeter (DSC) thermograms of Carboxymethyl Cellulose (CMC)-Amuniacum Gum (AMG)/Clove Essential Oil (CEO) films

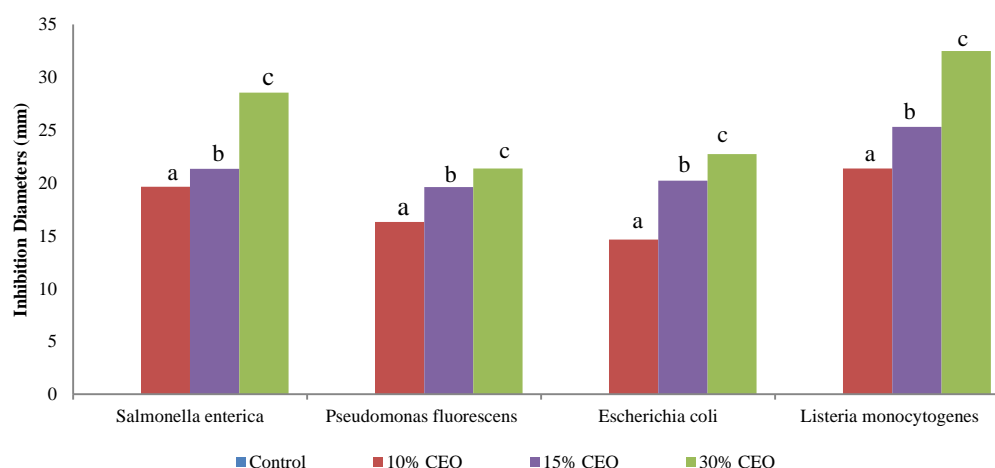


**Figure 6:** Antibacterial activity of the enriched Carboxymethyl Cellulose (CMC)-Amuniacum Gum (AMG) film with Clove Essential Oil (CEO). Different letters (a–c) indicate the significant differences ( $p < 0.05$ ). Values are expressed as mean  $\pm$  standard deviation

## Discussion

The results of thickness turned out to be in accordance with the finding of Walid et al. (2022) who verified that the thickness of the films projected no significant variation by incorporation of rosemary essential oil. Moreover, the identical results were reported by Shahbazi (2017) by incorporation of *Ziziphora clinopodioides* essential oil. In discordance with outcomes of the present study, Nisar et al. (2018) noticed that the thickness of the pectin film samples increased with the incorporation of CEO, ranging from 0.057 to 0.094 mm. The thickness of the film is influenced by the quantity of solid content available in the film-forming emulsion, as contrasted with control films in particular.

UTS is described as the maximum stress of a film that can be supported before breaking and SB estimates fracture toughness as a mechanical trait. For a given application in food packaging, some range of deformation is determined as mandatory prior to fracturing (Ebrahimi et al., 2022; Kadzińska et al., 2020). Similarly, Azarifar et al. (2019) reported that the addition of CMC into the gelatin-based nanocomposite film strengthened the film. Nisar et al. (2018) exposed that usage of 0–1.5% w/w CEO improved the UTS and SB in pectin films. At all levels of CMC and AMG, with an increase in CEO concentration, UTS reduced. This phenomenon in the film network considered to be the partial replacement of stronger polymer/polymer interactions with weak intermolecular polymer/CEO interactions, which decreased in the network cohesiveness



and UTS of the film (Araya et al., 2022). Alternatively, SB increased with the addition of CEO due to the presence of EOs as liquid at ambient temperature in the film structure which engendered an increase in film extensibility (Benavides et al., 2012). Correspondingly, Azarifar et al. (2019) reported that in gelatin-CMC films at all levels of *Trachyspermum ammi* (Ajowan) essential oil, UTS decreased and SB increased. With regard to Figure 1, the highest value of UTS (13.17 MPa) was obtained at 5% AMG, 1.5% CMC, and 15% CEO, while the maximum SB value (115.41%) was gained for 5% AMG, 1 % CMC, as well as 30% CEO formulations.

To maximize consumer acceptance, films color is regarded as a crucial factor since influence on the appearance of final product directly. The  $\Delta E$  values increased with the enhancement of CMC, AMG, and CEO concentrations. Hoque et al. (2011) declared that the addition of different herb extracts (cinnamon, clove, and star anise) to gelatin films led to a significant difference on the color by the increase of  $\Delta E$ . During film drying step lipid droplets induced coalescence and creaming, which promoted coarse surfaces by the presence of massive lipid molecules (Ghanbarzadeh and Almasi, 2011). Identical manners in reduction transparency were previously remarked for composite films containing EOs (Azarifar et al., 2019; Bertan et al., 2005; Ma et al., 2016). With addition of CMC, the film's optical characteristics can be notably improved which were determined similar to gelatin-based films reported by Azarifar et al. (2019). The maximum WI value (51.12) was obtained at 1% CMC, 1% AMG, and 0% CEO. In the current study, summary statistics were fulfilled and the results are displayed in Table 2, and also a list of suitable models in a coded form is observed in Table 3 that can accurately predict the formulation.

The FTIR peaks were perceived at 3,288 1/cm corresponded to the stretching vibrations of -OH, became almost flat and changed to 3,324 1/cm because of the increase in the concentration of CEO, indicating the decreased stretching of free O-H bonds affected by oil and CMC-AMG interaction (Yuen et al., 2009). Due to the presence of CEO, the bond region 2,800-2,900 1/cm transferred to 2,923 1/cm, pertinent to the aliphatic C-H stretching vibrational bands and denoting an increase in hydrophobicity of the film (Vlachos et al., 2006). The most intense absorption bonds were observed in the region between 1,760 and 800 1/cm which can be allocated to the phenolic groups, including carbonyl C=O absorptions in the region 1,712-1,704 1/cm and C=C stretching bonds at 1,612-1,608 and 1,519-1,516 1/cm (Lu et al., 2011). The peak at 1273 1/cm could be in spite of phenolic compounds and vibrations of the C-O stretch associated with polysaccharide (Cascant et al., 2016). Moreover, identical

spectral changes are discerned by Nisar et al. (2018) once incorporating clove bud essential oil in pectin films.

SEM was deployed to investigate the changes in the CMC-AMG film microstructure to administer useful information on distribution oil droplets within film matrix, and also its probable impact on the film properties. Obtained profound information of microstructural analysis related to the spatial arrangement in the film provides insight for better comprehension of the mass transfer mechanism and films' mechanical behavior (Vargas et al., 2009). Such a structural incoherence and heterogeneity at a higher percentage of EO would lead to a phase separation (oil and polymer) in the film matrix. Additionally, this type of roughness induced by the aggregates or droplets transmission toward the surface of films during drying progress has been resulted in surface irregularity (Bahrami and Fattahi, 2021). Prepared films with 15% w/w CEO displayed relatively smaller pores than the films with 30% w/w CEO and along with increasing oil amounts, the number of oil droplets heightened as well. A possible explanation for this phenomenon is associated with the oil droplet flocculation during drying with increasing droplet concentration, thus resulted in the formation of large size pores (Maleki and Mohsenzadeh, 2022). The SEM images definitely depicted the detrimental effect of CEO on the mechanical and barrier properties of the films. These findings align with a previous study conducted by Azarifar et al. (2019), which investigated gelatin-CMC films incorporating *Trachyspermum ammi* (Ajowan) essential oil. In contrast, Walid et al. (2022) declared varied results as incorporating rosemary essential oil into gelatin-chitosan films. In their study, no noticeable difference was observed between the SEM images of the control film as well as the film with rosemary essential oil, suggesting a potent interaction between rosemary essential oil and the biopolymers.

DSC studies of CMC-AMG films including various proportions of CEO were performed for additional information about thermally-induced intermolecular structural changes between polymers and CEO in Figure 5. The modification of thermal transitions occurs between 80-100 °C, were predominantly which invoked by the evaporation of water captured in the polymeric structure (Akhtar et al., 2018; Zhao et al., 2020). The endothermic peaks affected by the addition of CEO, therefore heat transitions shifted slightly to higher temperatures and ranged from 181.37 to 210 °C for 0 and 30% oil, respectively. The obtained results are in agreement with Radovic et al. (2019) which proved that incorporation of 56 mg of CEO/g had effect on the thermal stability of chitosan-gelatin blend films. Further, Nisar et al. (2018) identified that adding CEO from 0.5 to 1.5% enhanced the thermal stability of pectin films. The enhancement in

thermal stability can be connected to the interaction between film components and CEO which results in a denser matrix and a steadier network. The improvement can be related to the larger molecular weight and the hydrophobic traits of CEO as well.

Various antimicrobial compounds have been generated by plants against plant pathogenic bacteria that play an crucial role for resistance against microbial infections (Lin et al., 2004). Similar to our findings, Hosseini et al. (2009) reported inhibitory effects of CEO-containing chitosan films against *E. coli*, *L. monocytogenes*, and *S. aureus*. The eugenol followed by  $\beta$ -caryophyllen and acetaugenol were prominent components of CEO that induce inhibitory effects (Dashipour et al., 2014). EOs have the potential to disrupt the cytoplasmic membrane structure or other intracellular components and lead to lysis, cell depolarization, alteration membrane permeability by reducing cellular metabolic activities and eventually would die (Guo et al., 2021). The inhibitory effectiveness of the edible films incorporated with thyme and CEO against *L. monocytogenes* was also disclosed by Hosseini et al. (2009). Gram-positive bacteria (*L. monocytogenes*) seriously affected by the antimicrobial agent rather than the Gram-negative (*E. coli*) which the reason could be lied in their differences in the wall structure. Gram-positive bacteria prove to have a cell wall structure primarily composed of peptidoglycan and a slight amount of proteins. On the other hand, Gram-negative bacteria possess a lipid-rich cell wall composing of an outer membrane with various polysaccharides and proteins. This structural difference can restrict the penetration of hydrophobic compounds across the cell membrane in Gram-negative bacteria (Malanovic and Lohner, 2016; Matsuura, 2013). In contrast, Gram-positive bacteria without this barrier permit active compounds to easily enter the cell and inhibit or slow down bacterial growth (Vasconcelos et al., 2018).

## Conclusion

To discover the optimal design points of the CMC-AMG films enriched with CEO, an optimal mixture design method was utilized. Results were recommended that the combination of 1.5% CMC, 4.5% AMG, and 14.19% CEO were the optimal production conditions. Varying the ratio of CMC, AMG, and CEO ingredients in polymer matrices had a significant effect on the mechanical, color and antimicrobial characteristics of the subsequent CMC-AMG/CEO films. Adding CEO significantly diminished the UTS of the films; however thermal stability of the films was enhanced as illustrated by DSC analysis. The prosperous interaction among CMC, AMG, and the CEO was confirmed by FTIR. The antibacterial properties of the enriched CEO films were verified from disc diffusion

method against food-borne bacteria, including Gram-positive *L. monocytogenes*. The research outcomes projected that these films bear a significant potential as antimicrobial packaging to inhibit microbial growth and maintaining food quality. It was suggested that further studies focused on investigating the effects of these CMC-AMG based films on the water vapor permeability and improving their mechanical properties by adding various nanoparticles.

## Author contribution

A.H.R. study conception and design; K.A. analysis and interpretation of results; A.B. and T.F. draft manuscript preparation; E.B. conducted the experimental work. All authors read and approved the final manuscript.

## Conflict of interest

The authors declare that they do not have any conflict of interest.

## Acknowledgement

We appreciate for financial support of this work by Tabriz University of Medical Sciences, Tabriz, Iran (No. IR.TBZMED.VCR. REC.1397.438) and Food Biophysics Laboratory of Tabriz University.

## References

- Akhtar H.M.S., Riaz A., Hamed Y.S., Abdin M., Chen G., Wan P., Zeng X. (2018). Production and characterization of CMC-based antioxidant and antimicrobial films enriched with chickpea hull polysaccharides. *International Journal of Biological Macromolecules*. 118: 469-477. [DOI: 10.1016/j.ijbiomac.2018.06.090]
- Araya J., Esquivel M., Jimenez G., Navia D., Poveda L. (2022). Antimicrobial activity and physicochemical characterization of thermoplastic films based on bitter cassava starch, nanocellulose and rosemary essential oil. *Journal of Plastic Film and Sheeting*. 38: 46-71. [DOI: 10.1177/87560879211023882]
- American Society of Testing and Materials (ASTM) D882-02. (2002). Standard test method for tensile properties of thin plastic sheeting. URL: <https://www.astm.org/d0882-02.html>
- Azarifar M., Ghanbarzadeh B., Sowti Khiabani M., Akhondzadeh Basti A., Abdulkhani A., Noshirvani N., Hosseini M. (2019). The optimization of gelatin-CMC based active films containing chitin nanofiber and *Trachyspermum ammi* essential oil by response surface methodology. *Carbohydrate Polymers*. 208: 457-468. [DOI: 10.1016/j.carbpol.2019.01.005]
- Bahrani A., Fattahi R. (2021). Biodegradable carboxymethyl cellulose-polyvinyl alcohol composite incorporated with *Glycyrrhiza Glabra* L. essential oil: physicochemical and antibacterial features. *Food Science and Nutrition*. 9: 4974-4985. [DOI: 10.1002/fsn3.2449]
- Benavides S., Villalobos-Carvajal R., Reyes J.E. (2012). Physical, mechanical and antibacterial properties of alginate film: effect of the crosslinking degree and oregano essential oil concentration. *Journal of Food Engineering*. 110: 232-239. [DOI: 10.1016/

- j.foodeng.2011.05.023]
- Bertan L.C., Tanada-Palmu P.S., Siani A.C., Grosso C.R.F. (2005). Effect of fatty acids and 'Brazilian elemi' on composite films based on gelatin. *Food Hydrocolloids*. 19: 73-82. [DOI: 10.1016/j.foodhyd.2004.04.017]
- Bezerra M.A., Santelli R.E., Oliveira E.P., Villar L.S., Escalera L.A. (2008). Response surface methodology (RSM) as a tool for optimization in analytical chemistry. *Talanta*. 76: 965-977. [DOI: 10.1016/j.talanta.2008.05.019]
- Cascant M.M., Sisouane M., Tahiri S., EL Krati M., Cervera M.L., Garrigues S., De La Guardia M. (2016). Determination of total phenolic compounds in compost by infrared spectroscopy. *Talanta*. 153: 360-365. [DOI: 10.1016/j.talanta.2016.03.020]
- Dashipour A., Khaksar R., Hosseini H., Shojae-Aliabadi S., Ghanati K. (2014). Physical, antioxidant and antimicrobial characteristics of carboxymethyl cellulose edible film cooperated with clove essential oil. *Zahedan Journal of Research in Medical Sciences*. 16: 34-42.
- Ebrahimi B., Ghanbarzadeh B., Homayouni Rad A., Hemmati S., Moludi J., Arab K., Karimi S. (2022). Structural and physicochemical characterization of a novel water-soluble polysaccharide isolated from *Dorema ammoniacum*. *Polymer Bulletin*. 79: 9589-9608. [DOI: 10.1007/s00289-021-03952-y]
- Ebrahimi B., Homayouni Rad A., Ghanbarzadeh B., Torbati M., Falcone P.M. (2020). The emulsifying and foaming properties of Amuniacum gum (*Dorema ammoniacum*) in comparison with gum Arabic. *Food Science and Nutrition*. 8: 3716-3730. [DOI: 10.1002/fsn3.1658]
- Ebrahimi B., Mohammadi R., Rouhi M., Mortazavian A.M., Shojae-Aliabadi S., Koushki M.R. (2018). Survival of probiotic bacteria in carboxymethyl cellulose-based edible film and assessment of quality parameters. *LWT-Food Science and Technology*. 87: 54-60. [DOI: 10.1016/j.lwt.2017.08.066]
- Ghanbarzadeh B., Almasi H. (2011). Physical properties of edible emulsified films based on carboxymethyl cellulose and oleic acid. *International Journal of Biological Macromolecules*. 48: 44-49. [DOI: 10.1016/j.ijbiomac.2010.09.014]
- Gülçin İ., Şat İ.G., Beydemir Ş., Elmastaş M., Küfrevioğlu Ö.İ. (2004). Comparison of antioxidant activity of clove (*Eugenia caryophyllata* Thunb) buds and lavender (*Lavandula stoechas* L.). *Food Chemistry*. 87: 393-400. [DOI: 10.1016/j.foodchem.2003.12.008]
- Guo F., Chen Q., Liang Q., Zhang M., Chen W., Chen H., Yun Y., Zhong Q., Chen W. (2021). Antimicrobial activity and proposed action mechanism of linalool against *Pseudomonas fluorescens*. *Frontiers in Microbiology*. 12: 562094. [DOI: 10.3389/fmicb.2021.562094]
- Hoque S., Benjakul S., Prodpran T. (2011). Properties of film from cuttlefish (*Sepia pharaonis*) skin gelatin incorporated with cinnamon, clove and star anise extracts. *Food Hydrocolloids*. 25: 1085-1097. [DOI: 10.1016/j.foodhyd.2010.10.005]
- Hosseini M.H., Razavi S.H., Mousavi M.A. (2009). Antimicrobial, physical and mechanical properties of chitosan- based films incorporated with thyme, clove and cinnamon essential oils. *Journal of Food Processing and Preservation*. 33: 727-743. [DOI: 10.1111/j.1745-4549.2008.00307.x]
- Ju J., Xie Y., Guo Y., Cheng Y., Qian H., Yao W. (2019). Application of edible coating with essential oil in food preservation. *Critical Reviews in Food Science and Nutrition*. 59: 2467-2480. [DOI: 10.1080/10408398.2018.1456402]
- Kadzińska J., Bryś J., Ostrowska-Ligęza E., Estéve M., Janowicz M. (2020). Influence of vegetable oils addition on the selected physical properties of apple-sodium alginate edible films. *Polymer Bulletin*. 77: 883-900. [DOI: 10.1007/s00289-019-02777-0]
- Lin Y.T., Labbe R.G., Shetty K. (2004). Inhibition of *Listeria monocytogenes* in fish and meat systems by use of oregano and cranberry phytochemical synergies. *Applied and Environmental Microbiology*. 70: 5672-5678. [DOI: 10.1128/AEM.70.9.5672-5678.2004]
- Lu X., Wang J., Al-Qadiri H.M., Ross C.F., Powers J.R., Tang J., Rasco B.A. (2011). Determination of total phenolic content and antioxidant capacity of onion (*Allium cepa*) and shallot (*Allium oschaninii*) using infrared spectroscopy. *Food Chemistry*. 129: 637-644. [DOI: 10.1016/j.foodchem.2011.04.105]
- Ma Q., Zhang Y., Critzer F., Davidson P.M., Zivanovic S., Zhong Q. (2016). Physical, mechanical, and antimicrobial properties of chitosan films with microemulsions of cinnamon bark oil and soybean oil. *Food Hydrocolloids*. 52: 533-542. [DOI: 10.1016/j.foodhyd.2015.07.036]
- Malanovic N., Lohner K. (2016). Gram-positive bacterial cell envelopes: the impact on the activity of antimicrobial peptides. *Biochimica et Biophysica Acta (BBA)-Biomembranes*. 1858: 936-946. [DOI: 10.1016/j.bbamem.2015.11.004]
- Maleki M., Mohsenzadeh M. (2022). Optimization of a biodegradable packaging film based on carboxymethyl cellulose and Persian gum containing titanium dioxide nanoparticles and *Foeniculum vulgare* essential oil using response surface methodology. *Journal of Food Processing and Preservation*. 46: e16424. [DOI: 10.1111/jfpp.16424]
- Matsuura M. (2013). Structural modifications of bacterial lipopolysaccharide that facilitate Gram-negative bacteria evasion of host innate immunity. *Frontiers in Immunology*. 4: 109. [DOI: 10.3389/fimmu.2013.00109]
- Nisar T., Wang Z.-C., Yang X., Tian Y., Iqbal M., Guo Y. (2018). Characterization of citrus pectin films integrated with clove bud essential oil: physical, thermal, barrier, antioxidant and antibacterial properties. *International Journal of Biological Macromolecules*. 106: 670-680. [DOI: 10.1016/j.ijbiomac.2017.08.068]
- Pereda M., Ponce A.G., Marcovich N.E., Ruseckaite R.A., Martucci J.F. (2011). Chitosan-gelatin composites and bi-layer films with potential antimicrobial activity. *Food Hydrocolloids*. 25: 1372-1381. [DOI: 10.1016/j.foodhyd.2011.01.001]
- Radovic M., Adamovic T., Pavlovic J., Rusmirovic J., Tadic V., Brankovic Z., Ivanovic J. (2019). Supercritical CO<sub>2</sub> impregnation of gelatin-chitosan films with clove essential oil and characterization thereof. *Chemical Industry and Chemical Engineering Quarterly*. 25: 119-130. [DOI: 10.2298/CICEQ180323025R]
- Raeisi M., Tajik H., Aliakbarlu J., Mirhosseini S.H., Hosseini S.M.H. (2015). Effect of carboxymethyl cellulose-based coatings incorporated with *Zataria multiflora* Boiss. essential oil and grape seed extract on the shelf life of rainbow trout fillets. *LWT-Food Science and Technology*. 64: 898-904. [DOI: 10.1016/j.lwt.2015.06.010]
- Salama H.E., Abdel Aziz M.S., Sabaa M.W. (2019). Development of antibacterial carboxymethyl cellulose/chitosan biguanidine hydrochloride edible films activated with frankincense essential oil. *International Journal of Biological Macromolecules*. 139: 1162-1167. [DOI: 10.1016/j.ijbiomac.2019.08.104]
- Shahbazi Y. (2017). The properties of chitosan and gelatin films incorporated with ethanolic red grape seed extract and *Ziziphora clinopodioides* essential oil as biodegradable materials for active food packaging. *International Journal of Biological Macromolecules*. 99: 746-753. [DOI: 10.1016/j.ijbiomac.

- 2017.03.065]
- Vargas M., Albors A., Chiralt A., González-Martínez C. (2009). Characterization of chitosan–oleic acid composite films. *Food Hydrocolloids*. 23: 536-547. [DOI: 10.1016/j.foodhyd.2008.02.009]
- Vasconcelos N.G., Croda J., Simionatto S. (2018). Antibacterial mechanisms of cinnamon and its constituents: a review. *Microbial Pathogenesis*. 120: 198-203. [DOI: 10.1016/j.micpath.2018.04.036]
- Vlachos N., Skopelitis Y., Psaroudaki M., Konstantinidou V., Chatzilazarou A., Tegou E. (2006). Applications of fourier transform-infrared spectroscopy to edible oils. *Analytica Chimica Acta*. 573-574: 459-465. [DOI: 10.1016/j.aca.2006.05.034]
- Walid Y., Malgorzata N., Katarzyna R., Piotr B., Ewa O.-L., Izabela B., Wissem A.-W., Majdi H., Slim J., Karima H.-N., Dorota W.-R., Moufida S.-T. (2022). Effect of rosemary essential oil and ethanol extract on physicochemical and antibacterial properties of optimized gelatin–chitosan film using mixture design. *Journal of Food Processing and Preservation*. 46: e16059. [DOI: 10.1111/jfpp.16059]
- Yeddes W., Djebali K., Wannes W.A., Horchani-Naifer K., Hammami M., Younes I., Tounsi M.S. (2020). Gelatin-chitosan-pectin films incorporated with rosemary essential oil: optimized formulation using mixture design and response surface methodology. *International Journal of Biological Macromolecules*. 154: 92-103. [DOI: 10.1016/j.ijbiomac.2020.03.092]
- Yuen S.-N., Choi S.-M., Phillips D.L., Ma C.-Y. (2009). Raman and FTIR spectroscopic study of carboxymethylated non-starch polysaccharides. *Food Chemistry*. 114: 1091-1098. [DOI: 10.1016/j.foodchem.2008.10.053]
- Zhao F., Guo Y., Zhou X., Shi W., Yu G. (2020). Materials for solar-powered water evaporation. *Nature Reviews Materials*. 5: 388-401. [DOI: 10.1038/s41578-020-0182-4]